

*SOFT, Rostock, Germany, 15.-19. September 2008*

**MECHANICAL AND THERMO-PHYSICAL CHARACTERIZATION OF 3-DIRECTIONAL CARBON FIBER COMPOSITES FOR W-7X AND ITER**

G. Pintsuk<sup>a\*</sup>, J. Compan<sup>a</sup>, T. Koppitz<sup>a</sup>, J. Linke<sup>a</sup>, A.T. Peacock<sup>b</sup>, D. Pitzer<sup>a</sup>,  
M. Rödiger<sup>a</sup>, S. Wikman<sup>c</sup>

<sup>a</sup> *Forschungszentrum Jülich GmbH, Euratom Association, D-52425 Jülich, Germany*

<sup>b</sup> *Max-Planck-Institut für Plasmaphysik, Euratom Association, D-85748 Garching,  
Germany*

<sup>c</sup> *Fusion For Energy, E-08019 Barcelona, Spain*

**Abstract**

Carbon fiber composites (CFCs) are the first choice as plasma facing materials for the strike points of divertor targets for future nuclear fusion devices like WENDELSTEIN 7-X and ITER. For the application in these facilities several potential European 3D-CFCs were compared and qualified: 1) four material batches of NB31 produced by Snecma Propulsion Solide (SNECMA); 2) NB41, SNECMA, the upgraded version of NB31; 3) N31, SNECMA, which is densified by chemical vapor infiltration (CVI) instead of a final liquid pitch infiltration characteristic for NB31; 4) a new developmental 3D-CFC produced by DUNLOP.

The characterization of the composites is comprised of thermo-physical measurements and tensile tests. The results are correlated to density and microstructure and summarized as follows: 1) NB41 provides the highest thermal conductivity in the ex-pitch direction of  $\sim 375$  W/m.K at room temperature; 2) all material grades are, due to their heterogeneity, characterized by a relatively large scatter of mechanical properties; 3) the different densification process for N31 in comparison to NB31 has no influence on the material properties; 4) NB41 provides in all 3 directions a comparably high tensile strength with an average in the ex-pitch direction of  $\sim 220$  MPa; 5) the 3D-

***SOFT, Rostock, Germany, 15.-19. September 2008***

CFC from DUNLOP is comparable to NB41 but yet does not meet the specifications in the needling direction.

*Keywords: CFC, tensile strength, thermal conductivity*

*\*Corresponding author: e-mail: [g.pintsuk@fz-juelich.de](mailto:g.pintsuk@fz-juelich.de)*

*Tel.: +49-(0)2461-616300*

*Fax.: +49-(0)2461-613699*

*Forschungszentrum Jülich, IEF-2*

*52425 Jülich*

*Germany*

## **1 Introduction**

Although carbon fiber composites (CFCs) provide detrimental material behavior in combination with tritium and related neutron irradiation, CFCs as plasma facing materials in actual and future experimental nuclear fusion devices are still of significant importance. This is based on their excellent thermal shock resistance [1,2], absence of melting in comparison with metals and ability to retain the strength up to high temperatures [3,4]. These are desirable properties for the strike point area of the ITER divertor during the start-up phase without tritium [5-7] as well as for the divertor of WENDELSTEIN 7-X [8,9].

One of the main issues in the development of divertor components for those devices is the definition of material requirements for plasma facing materials. These have to fulfill the occurring manufacturing and operational needs which is nowadays also a matter of numerical simulations [5,10]. Among these materials are several CFCs, for which the characterization results are summarized in [11,12]. The variations in microstructural and material properties for the individual material grades are quite large and each of these providing specific advantages and disadvantages. Therefore the main aim of the European fusion program was to define the properties of a reference material and material structure, i.e. NB31. With this definition the design and production technology, e.g. the densification and needling process, could be optimized. Nevertheless also among the different batches of NB31, which should be microstructurally equivalent, strong variations take place due to the heterogeneity and the complex manufacturing process of the CFCs.

Therefore within the frame of this work several potential European 3 directional (3D) CFCs with similar structures of orthogonal ex-pitch, ex-PAN and needling orientation, were compared: 1) four material batches of NB31, the actual European standard and reference material produced by Snecma Propulsion Solide (SNECMA),

called “pilot”, “serial”, “additional” (see [13]) and the latest one “extra” production; 2) NB41, SNECMA, the upgraded version of NB31 and its potential successor; 3) N31, SNECMA, which is missing the final liquid pitch infiltration characteristic for NB31 and is densified by the cheaper chemical vapor infiltration (CVI) process only; 4) a new developmental 3D-CFC produced by DUNLOP with similar fiber types and architectures to the SNECMA materials. The amount of fabricated material varied between tenths and hundreds (for NB31, “serial” and “additional” production) of kilogram. For WENDELSTEIN 7-X the selected material NB31 was already delivered whose finalized characterization results are presented herein. The material selection for the European contribution to the ITER divertor is still ongoing and NB41, N31 as well as the DUNLOP material are potential candidates.

## **2 Material and Characterization**

### **2.1 Material**

The four investigated material grades, i.e. NB31, N31, NB41 and the developmental DUNLOP CFC, are 3D materials with the fibers oriented in the 3 orthogonal spatial directions. With regard to fusion applications the fibers oriented in the high heat flux direction are made of pitch precursors while in the other two directions the fibers used are PAN-fibers. In particular the fibers are forming a 2D laminar structure consisting of ex-pitch and ex-PAN fiber layers which is then reinforced in the third direction by a so-called needling process. This is causing the reorientation of a part of the ex-PAN fibers, which provide a higher flexibility than the ex-pitch fibers.

The microstructure of the materials differs between the material grades but also between the different batches of NB31 due to a variation in fiber planes per volume. The combination of an ex-pitch fiber layer with an ex-PAN fiber layer has been defined

as “unit cell”. Their combined width as well as the ratio between ex-pitch and unit cell width (pitch ratio) define characteristic parameters of the fiber reinforced material, which can be determined easily by optical micrographs from the outer surface of the produced CFC-blocks (see Tab. 1). Both parameters vary significantly between the different materials and even between the different batches of NB31. Beside a change of the unit cell width also a variation of the amount and length of needling fibers was observed. This was determined to be least for the developmental DUNLOP CFC and highest for the serial production of NB31 which has a direct influence not only on the materials microstructure but also on the mechanical properties (see chapter 3).

Also shown in Tab. 1 are the density ranges for the different materials, which were determined by weight and size measurements of the thermal diffusivity specimens (see chapter 2.2). These were cut out from different positions within the delivered blocks. Due to their small dimensions they perfectly represent the density distribution and highlight the density gradient from the surface to the center of the CFC-blocks, which is a result of the manufacturing process. Accordingly, NB41 with the highest pitch ratio provides the highest density among the different grades. N31, as a result of the different final densification process in comparison to NB31, and the DUNLOP CFC are showing the lowest values. Since the dimensions of the delivered blocks were quite similar, an influence of this parameter on the density gradient could not be determined. However, based on the manufacturing process larger dimensions are expected to result in a broader density distribution.

## 2.2 Thermo-physical and mechanical characterization

The determination of the thermal conductivity is based on the measurement of the thermal diffusivity  $a$ . In combination with the density  $\rho$  and the specific heat  $c_p$  of

the material, the thermal conductivity  $\lambda$  can be calculated from the equation as a function of the temperature T:

$$\lambda(T) = a(T) \cdot \rho(T) \cdot c_p(T) \quad (1)$$

For the measurement of the thermal diffusivity, depending on the batch, one to three specimens with a diameter of 10 mm and a height of 5 mm were measured per fiber orientation. The experiments were performed in the temperature range between room temperature and 1200°C in intervals of 200°C. In the same temperature range heat capacities were determined on cylindrical specimens with a diameter of 5 mm and a height of 1 mm taking care of a representative distribution of ex-pitch and ex-PAN fibers in the specimens. Furthermore CTE measurements were performed by pull-rod dilatometry on NB41 and the new DUNLOP CFC using cylindrical specimens of 4 mm in diameter and 25 mm in length. The investigated temperature range was 200-900°C.

The tensile tests at room temperature were performed on two types of tensile test specimens, flat dog bone and dumbbell shaped (see Fig. 1). This resulted from the different dimensions of the particular CFC-blocks that made it necessary to adapt the cutting plan and especially the tensile test specimen geometry to the given boundary conditions. The goal was to get a maximum number of specimens necessary for the reliable and statistical characterization of this brittle material by staying as close as possible to the EUROPEAN STANDARD EN 658-1.

The tests for the pilot and serial productions of NB31 were performed strain controlled whereas the tests for all other materials were conducted stress controlled. This resulted into more clearly defined stress-strain relationships in contrast to the strain controlled measurements. The maximum reached load was used to calculate the tensile strength and from the initial slope of the curve the Young's modulus was determined.

Using Weibull statistics, which is based on the concept of the failure of the weakest link, the strength distribution of the CFC was described effectively in mathematical terms (see equation 2) by the distribution function F:

$$F(V, \sigma) = 1 - \exp\left\{-\left(V/V_0\right) \cdot \left(\sigma/\sigma_0\right)^m\right\}$$
$$\ln\left\{\ln\left(1/(1-F)\right)\right\} = \ln\left(V/V_0\right) + m \cdot \ln(\sigma) - m \cdot \ln(\sigma_0) \quad (2)$$

Therein  $m$  is the Weibull modulus and  $\sigma_0$  and  $\sigma$  are the normalized stress and the stress at failure, respectively.  $V$  and  $V_0$  are the affected specimen volume and the reference volume. Since the affected cross section and volume of the specimens were almost constant for the particular directions, in an approximation the term  $\ln(V/V_0)$  was set to 0. This results in a defined relationship between the mechanical load and the failure probability of a part if the distribution parameters are known. The Weibull modulus itself is a measure of the distribution of strengths and the higher the Weibull modulus, the higher the consistency of the material (which means that uniform "defects" are evenly distributed throughout the entire volume). Ideally a material has an endless Weibull modulus but due to the brittleness of ceramics they are typically providing values between  $10 < m < 20$ .

A detailed description of the set-up for the thermo-physical and the mechanical testing can be found in [13].

### **3 Results and Discussion**

The obtained results on the thermo-physical and mechanical properties will be addressed from two different points of view: 1) the material development for ITER which is still ongoing and that's why some materials are still in the developmental stage

(e.g. DUNLOP); 2) the material qualification for the manufacturing of divertor components for WENDELSTEIN 7-X. The latter comprises all batches of NB31 and in case of the serial and additional production those dedicated for the “IPP”.

In Tab. 2 and Tab. 3 the main determined thermo-physical and mechanical properties are summarized and will in the following be qualified and correlated to the microstructure. This is essential for the better understanding of the material’s behavior and its optimization. The specific heat listed in Tab. 2 in dependence of temperature shows only slight variations between the different CFC grades leading to the assumption of a rather constant specific heat. This is due to its similarity to NB31 also valid for N31, which was not explicitly characterized. Especially NB41 and the DUNLOP material show a remarkable close overlapping. With regard to thermal conductivity, which determines the heat removal capacity, the surface temperature and subsequently the erosion lifetime of the component are characterizing the investigated CFCs:

a) As has been found in [13, 14], an increasing density results in an increase of thermal conductivity up to a certain saturation value. If the threshold for reaching this saturation is exceeded, the standard deviation of the measured thermal conductivity values reduces to a minimum. This is dependent on the scatter at each individual density level. In case of the investigated materials only the NB31 pilot production did not and the new DUNLOP material do not yet provide a density range fully above this threshold, which is about  $1.86 \text{ g/cm}^3$  for NB31 and  $\sim 1.8 \text{ g/cm}^3$  for the DUNLOP material.

b) Important for WENDELSTEIN 7-X, the different batches of NB31 show among them no relevant difference in thermal conductivity in any of the three orthogonal directions. Nevertheless the evaluation of the serial production made for EFDA and not for WENDELSTEIN 7-X shows a lower value ( $\Delta\lambda \approx 25\text{-}30 \text{ W/m.K}$ ).



This is resulting from the microstructural modifications, i.e. the reduction in unit cell width, the increase in needling fibers and the increased damage of pitch fibers and fiber bundles.

c) N31 with a final CVI process instead of a liquid pitch infiltration is equivalent to NB31 even with the lower achieved density values shown in chapter 2.1 which therefore are assumed to be above the threshold value.

d) In the ex-pitch direction NB41 offers the highest thermal conductivity among all tested CFC grades. This directly correlates with the microstructure, i.e. the highest pitch ratio providing an increased amount of pitch fibers and correlated to this a higher amount of highly oriented graphite matrix in the high heat flux direction.

Furthermore lower modulus pitch fibers were used with simplified fiber architecture expected to give improved properties. Correspondingly the thermal conductivity in the other two directions is, due to the lower amount of PAN-fibers per volume, reduced in comparison to NB31 and N31.

e) The developmental DUNLOP CFC provides similar thermal conductivity values than NB31 except for the needling direction for which it only achieves half of the thermal conductivity of all other CFCs. This results from a not yet optimized needling reinforcement which is also expressed in a significant increase in CTE in the needling direction in comparison to NB41 (see Fig. 2).

Beside good thermo-physical properties, the CFCs also have to provide a high mechanical strength to sustain the residual stresses formed by the manufacturing process as well as the thermally induced stresses during operation. Since for CFCs as a general rule material strengthening takes place up to temperatures of 1500-2000°C a sufficient and reliable material characterization can be limited to the determination of RT values. Temperatures up to 2000°C also correspond to the maximum standard

operational temperatures of CFCs in the divertor region of a fusion device. Nevertheless due to the heterogeneity of the materials a broad band of measurement results, typical for a brittle material, were generated. Therefore a sufficient amount of material data was necessary to qualify the material. Due to a limited and depending on the material batch and grade varying amount of available material, the results were obtained by testing a minimum of 4 up to 24 tensile specimens.

In the following the determined mechanical properties (see Tab. 3 and Fig. 3) and the found correlations and drawn conclusions are summarized:

a) As a consequence of the microstructural variations outlined in chapter 2.1 for the different batches of NB31 a decrease in tensile strength in the ex-pitch direction is correlated with an increase of the strength in the needling direction. The strength in needling direction achieves a maximum of ~19-26 MPa for the serial production with the lowest unit cell width and the highest pitch ratio. This leads to the conclusion that for NB31 by a larger unit cell width in combination with a lower pitch ratio a better mechanical performance is achieved. Nevertheless, the significant variation by a factor 2-3 in mechanical properties in dependence of the material batch (see Fig. 3 top; ex-pitch direction) increases the necessary efforts for reliable manufacturing, operation and life time prediction of fusion components.

b) As already been found for the thermo-physical properties N31 shows also similar mechanical properties as NB31, even with a lower final density. Therefore from this point of view the different densification processes have to be regarded as equivalent.

c) In contradiction to the findings for NB31, for NB41 a higher unit cell width and pitch ratio in comparison to NB31 results in about double the tensile strength in the ex-pitch direction without losing the good properties in the other directions. This indicates that an optimization of the manufacturing process and of the used preform has

taken place. In it the ex-pitch fibers and the overall microstructural design are less affected by the needling process guaranteeing a good reproducibility.

d) Similar to NB41, the new but still developmental DUNLOP CFC also shows the same microstructural and tensile strength characteristics for the ex-pitch and the ex-PAN direction. Like for the thermal conductivity and because of the same reasons, a very low strength in the needling direction is obtained. After an enhancement of the manufacturing optimized material properties are expected for the next batches that have been already produced.

e) By plotting tensile strength as a function of Young's modulus as it is done in Fig. 3 by introducing the medium values and the respective standard deviations two separate linear relationships between the different CFC batches and grades were found. On the one hand the results for the ex-pitch fiber directions of the different SNECMA materials are correlated by a linear relation providing a slope of  $\sim 1.27 \cdot 10^{-3}$ . The correlation does not comprise the results for the DUNLOP CFC which shows, in comparison to the SNECMA grades, a higher tensile strength already at a lower Young's modulus, indicating different material properties of the used ex-pitch fibers. In the bottom graph of Fig. 3 the results for the ex-PAN fiber directions of the SNECMA materials are highlighted showing a combined slope of  $2.55 \cdot 10^{-3}$ . This is about double as high as for the ex-pitch fiber direction outlining that for the ex-PAN fibers the influence of stiffness on the mechanical strength is significantly higher than for the ex-pitch fibers. In contrast to the ex-pitch fiber directions these results are in good agreement to those for the ex-PAN fiber directions of the DUNLOP CFC.

As mentioned before, the heterogeneity of the materials and their brittleness generated a broad band of measurement results. Such materials are characterized most effectively by using Weibull statistics for which about 30 samples are recommended

(European Prestandard ENV 843-5). Since this is above the amount of available and used specimens (see above) the obtained results have to be handled with care.

Nonetheless the determined parameters, Weibull modulus and normalized stress (see Tab. 4), were finally used to calculate the failure probability for the particular directions. This means the percentage of specimens failing at a certain stress level. This is here outlined by concentrating on the ex-pitch direction (see Fig. 4), showing a clear ranking among the different batches of NB31. The comparison of NB41 and the DUNLOP CFC shows no clear advantage for any of them. DUNLOP offers a better performance above 200 MPa while the failure probability stays longer below a certain threshold value for NB41, e.g. 1% failure probability is achieved at about 164 MPa for NB41 while the DUNLOP CFC achieves it already at 138 MPa. Remembering the rather low amount of tested specimens, further investigations for a final qualification have to be done in the future.

#### **4 Conclusion**

Four batches of CFC SEPCARB<sup>®</sup> NB31, namely the pilot, serial, additional and extra production, N31, NB41 and a developmental DUNLOP CFC have been thermo-physically and mechanically characterized. The obtained results were correlated to the microstructure, which consists of similar or even identical constituents but nevertheless provides significant differences among the material grades on a microstructural scale.

The microstructural differences and a related change in manufacturing technology mainly result in a modification of the mechanical properties of the investigated materials. Density has no absolute but only a relative influence which is related to the applied densification process. The latter is expressed by the fact that N31 (CVI densification) with an average density  $\sim 0.8 \text{ g/cm}^3$  lower than those for NB31 (liquid pitch infiltration), extra production, offers the same mechanical properties. In

contrast, the thermo-physical characteristics of the CFCs are hardly affected by microstructure. Only for NB41 the increased amount of undamaged fibers in the ex-pitch direction lead to an increase in thermal conductivity up to  $\sim 375$  W/m.K in comparison to about 300 W/m.K for all other investigated CFC grades. Among all investigated materials, it is also NB41 provides the best combination of thermo-physical and mechanical properties in all three orthogonal directions. However, a statement on the stability of NB41 as it was done for NB31 is, based on the presented work, not possible due to the testing of a single batch only.

## **5 Acknowledgement**

This work, supported by the European Communities under the contract of Association between EURATOM/FZJ, was carried out within the framework of the European Fusion Development Agreement. The views and opinions expressed herein do not necessarily reflect those of the European Commission.

## **6 References**

- [1] G. Federici, A. Zhitlukhin, N. Arkhipov, R. Giniyatulin, N. Klimov, I. Landman, V. Podkovyrov, V. Safronov, A. Loarte, M. Merola; Effects of ELMs and disruptions on ITER divertor armour materials, *J. Nucl. Mat.* 337-339 (2005) 684-690
- [2] S. Pestchanyi, V. Safronov, I Landman; Estimation of carbon fibre composites as ITER divertor armour, *J. Nucl. Mat.* 329-333 (2004) 697-701
- [3] G. Kalinin, V. Barabash, A. Cardella, J. Dietz, K. Ioki, R. Matera, R.T. Santoro, R. Tivey, The ITER Home Teams; Assessment and selection of materials for ITER in-vessel components, *J. Nucl. Mat.* 283-287 (2000) 10-19

- [4] T. Tanabe; On the possibility of ITER starting with full carbon, *Fus. Eng. Des.* 81 (2006) 139-147
- [5] M. Merola, W. Dänner, M. Pick; EU R&D on divertor components, *Fus. Eng. Des.* 75-79 (2005) 325-331
- [6] M. Missirlian, F. Escourbiac, M. Merola, I. Bobin-Vastra, J. Schlosser, A. Durocher; Results and analysis of high heat flux tests on a full-scale vertical target prototype of ITER divertor, *Fus. Eng. Des.* 75-79 (2005) 435-440
- [7] S. Fouquet, J. Schlosser, M. Merola, A. Durocher, F. Escourbiac, A. Grosman, M. Missirlian, C. Portafaix; Acceptance criteria for the ITER divertor vertical target, *Fus. Eng. Des.* 81 (2006) 265-268
- [8] J. Boscary, H. Greuner, B. Mendelevitch, B. Schedler, K. Scheiber, J. Schlosser, B. Streibl; Applied technologies and inspections for the W7-X pre-series target elements, *Fus. Eng. Des.* 75-79 (2005) 451-455
- [9] J. Boscary, B. Böswirth, H. Greuner, M. Missirlian, B. Schedler, K. Scheiber, J. Schlosser, B. Streibl; Results of the examinations of the W7-X pre-series target elements, *Fus. Eng. Des.* 82 (2007) 1634-1638
- [10] A. Plankensteiner, A. Leuprecht, B. Schedler, K.-H. Scheiber, H. Greuner; Finite element based design optimization of WENDELSTEIN 7-X divertor components under high heat flux loading, *Fus. Eng. Des.* 82 (2007) 1813-1819
- [11] ITER: Material Assessment Report (MAR), April 2004, G 74 MA 10 W 0.3
- [12] A.T. Peacock, M. Merola, M.a. Pick, R. Tivey; Status of CFC development in Europe for ITER, *Phys. Scr.* T128 (2007) 23-28
- [13] G. Pintsuk, J. Compan, J. Linke, P. Majerus, A. Peacock, D. Pitzer, M. Rödiger; Mechanical and thermo-physical characterization of the carbon fibre composite NB31, *Phys. Scr.* T128 (2007) 66-71

- [14] M. Lipa, P. Chappuis, G. Chaumat, D. Guilhem, R. Mitteau, L. Plöchl;  
Development and fabrication of improved CFC-brazed components for the inner  
first wall of Tore Supra, Proc. 19<sup>th</sup> SOFT, Lisbon (1996) 439-442





**List of pictures**

Fig. 1: Concept of tensile test specimens; a) dogbone and b) dumbbell geometry

Fig. 2: Coefficient of thermal expansion for NB41 and the DUNLOP-CFC in the three orthogonal spatial directions

Fig. 3: Tensile strength as a function of Young's modulus; medium values with standard deviation for all directions (top) and for the ex-PAN and the needling directions in particular (bottom)

Fig. 4: Failure probability for the ex-pitch direction of the different CFCs as a function of occurring stress concentration

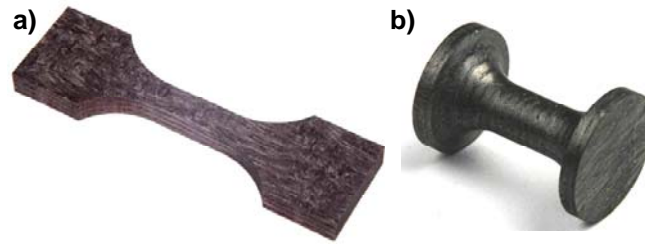


Fig. 1: Concept of tensile test specimens – a) dogbone and b) dumbbell geometry

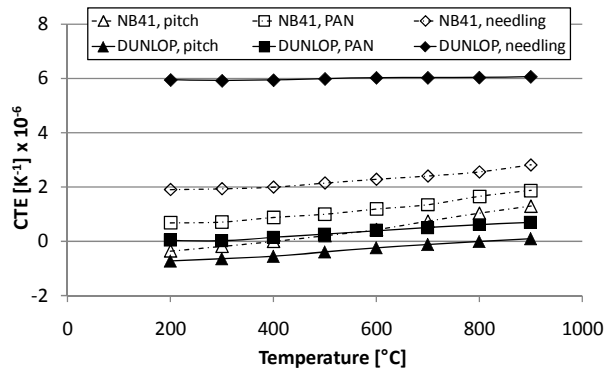


Fig. 2: Coefficient of thermal expansion for NB41 and the DUNLOP-CFC in the three orthogonal spatial directions

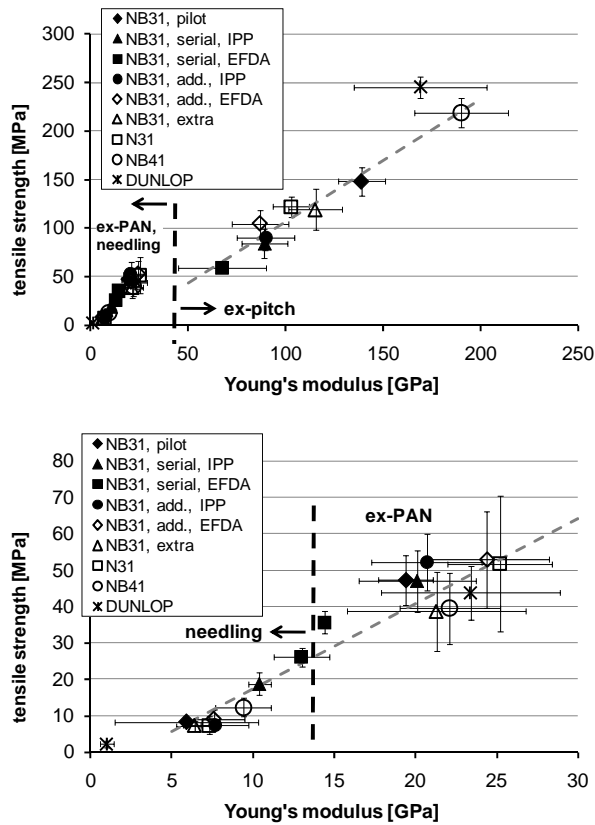


Fig. 3: Tensile strength as a function of Young's modulus; medium values with standard deviation for all directions (top) and for the ex-PAN and the needling directions in particular (bottom) – linear relationships for the ex-pitch and the ex-PAN directions

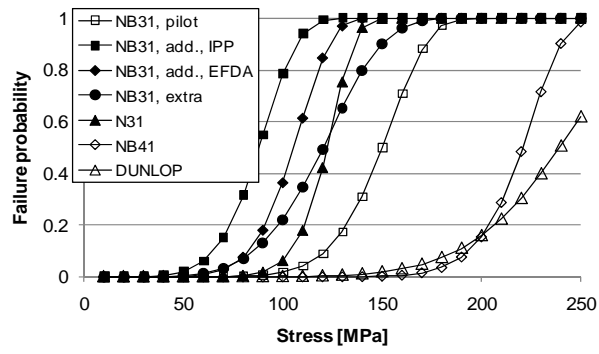


Fig. 4: Failure probability for the ex-pitch direction of the different CFCs as a function of occurring stress concentration

**List of tables**

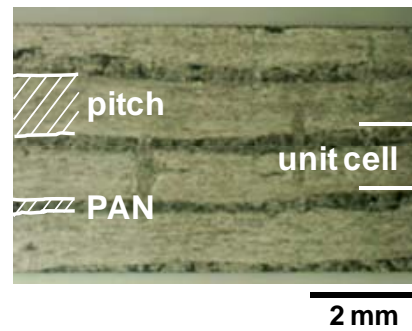
Tab. 1: Density and variables of the microstructural assembly; stereomicroscopic image of NB41

Tab. 2: Specific heat of the different CFCs as a function of temperature

Tab. 3: Thermo-physical and mechanical properties (average values with standard deviation) of all investigated CFCs

Tab. 4: Weibull moduli and normalized stress for the 3 orthogonal directions of the investigated CFCs

<b>material</b>	<b>density range [g/cm<sup>3</sup>]</b>	<b>unit cell [mm]</b>	<b>pitch ratio [%]</b>
<b>NB31, pilot</b>	1.84 – 1.96	1.67	56
<b>NB31, serial</b>	1.93 – 1.96	1.33	70
<b>NB31, add.</b>	1.87 – 1.98	1.47	63
<b>NB31, extra</b>	1.91 – 1.96	1.45	56
<b>N31</b>	1.81 – 1.89	1.45	56
<b>NB41</b>	1.94 – 2.00	1.3	77
<b>DUNLOP</b>	1.75 – 1.88	0.94	70



Tab. 1: Density and variables of the microstructural assembly; stereomicroscopic image of NB41

<b>material</b>	<b>specific heat [J/kg.K]</b>		
	<b>200°C</b>	<b>800°C</b>	<b>1000°C</b>
<b>NB31</b>	1121	1860	1938
<b>NB41</b>	1143	1807	1876
<b>DUNLOP</b>	1162	1797	1877

Tab. 2: Specific heat of the different CFCs as a function of temperature



		NB31, pilot	NB31, serial, IPP	NB31, serial, EFDA	NB31, add., IPP	NB31, add., EFDA	NB31, extra	N31	NB41	DUNLOP
		<b>ex-pitch</b>								
therm. cond. [W/m.K]	RT	290 $\pm 23.6$	306.8 $\pm 0.5$	277.5 $\pm 9.7$	308.5 $\pm 3.9$	302.2 $\pm 5.1$	306.4 $\pm 10.3$	312 $\pm 4.6$	375.3 $\pm 8.1$	293 $\pm 47$
	800°C	161 10.6	172.2 $\pm 2.3$	157.8 $\pm 1.4$	172.7 $\pm 3.8$	170 $\pm 5.4$	174 $\pm 6.9$	176.2 $\pm 0.1$	197.4 $\pm 6.7$	173.2 $\pm 19$
Young's mod. [GPa]	RT	139 $\pm 12.6$	89.2 $\pm 11.9$	67.4 $\pm 22.4$	89.7 $\pm 19.1$	87 $\pm 14.7$	115.3 $\pm 13.9$	102.8 $\pm 9.2$	190 $\pm 24$	169.1 $\pm 34.1$
tensile strength [MPa]	RT	148 $\pm 12.3$	83.9 $\pm 14.9$	58.8 $\pm 3.1$	89 $\pm 15.8$	104.5 $\pm 13.6$	119.1 $\pm 21.1$	121.9 $\pm 10.5$	219.2 $\pm 15$	245.1 $\pm 11$
		<b>ex-PAN</b>								
therm. cond. [W/m.K]	RT	109 $\pm 14.7$	110.1 $\pm 8.5$	91.2 $\pm -$	109.3 $\pm 4.8$	115.5 $\pm 2.6$	112.1 $\pm 5$	107.4 $\pm -$	99.5 $\pm 6.6$	113.1 $\pm 22.1$
	800°C	59.3 $\pm 3.5$	63 $\pm 1.1$	54.9 $\pm -$	64 $\pm 1$	67.4 $\pm 2.4$	66.4 $\pm 1$	63.4 $\pm -$	59.2 $\pm 2.6$	63 $\pm 8.3$
Young's mod. [GPa]	RT	19.4 $\pm 1.7$	20.1 $\pm 3.6$	14.4 $\pm 0.3$	20.7 $\pm 3.4$	24.4 $\pm 3.8$	21.3 $\pm 5.5$	25.2 $\pm 3.2$	22.1 $\pm 3.1$	23.4 $\pm 5.5$
tensile strength [MPa]	RT	47.3 $\pm 6.8$	47 $\pm 8.4$	35.6 $\pm 3.1$	52.5 $\pm 7.8$	52.9 $\pm 13.2$	38.7 $\pm 10.8$	51.8 $\pm 18.7$	39.5 $\pm 9.7$	43.8 $\pm 7.3$
		<b>Needling</b>								
therm. cond. [W/m.K]	RT	86 $\pm 4.5$	96.7 $\pm 0.8$	89.3 $\pm -$	83 $\pm 1.3$	80.5 $\pm 3.4$	81.9 $\pm 4$	85.9 $\pm -$	74.8 $\pm 3.2$	47.8 $\pm 11.6$
	800°C	45 $\pm 2$	52.1 $\pm 1.7$	48.8 $\pm -$	47.4 $\pm 0.4$	44.4 $\pm 3.4$	48 $\pm 2.5$	46.3 $\pm -$	43.8 $\pm 1.8$	27.2 $\pm 7.7$
Young's mod. [GPa]	RT	5.9 $\pm 4.4$	10.4 $\pm 0.7$	13 $\pm 1.7$	7.7 $\pm 2$	7.6 $\pm 1.9$	6.4 $\pm 1.1$	7.3 $\pm 0.5$	9.4 $\pm 1.7$	1.0 $\pm 0.4$
tensile strength [MPa]	RT	8.3 $\pm 0.6$	18.8 $\pm 3.2$	26.1 $\pm 2.6$	7.4 $\pm 1.4$	9.1 $\pm 2.6$	7.2 $\pm 1.3$	7.4 $\pm 2.4$	12.3 $\pm 2.6$	2.2 $\pm 0.9$

Tab. 3: Thermo-physical and mechanical properties (averages with standard deviation) of all investigated CFCs

	NB31, pilot	NB31, add., IPP	NB31, add., EFDA	NB31, extra	N31	NB41	DUNLOP
	<b>ex-pitch</b>						
<b>Weibull mod.</b>	9.0	6.3	7.8	5.5	11.7	14.4	7.7
<b>norm. stress [MPa]</b>	156.4	93.4	110.7	128.6	126.3	226.4	251.1
	<b>ex-PAN</b>						
<b>Weibull mod.</b>	6.7	6.9	4.6	3.1	1.9	3.6	6.7
<b>norm. stress [MPa]</b>	49.1	55.7	59.3	43.6	61.8	44.0	47.8
	<b>needling</b>						
<b>Weibull mod.</b>	9.7	4.6	2.9	3.7	5.1	4.8	2.1
<b>norm. stress [MPa]</b>	8.7	8.1	10.3	8.5	7.0	13.4	2.6

Tab. 4: Weibull moduli and normalized stress